Supplemental Information

Role of Hsc70 Binding Cycle in CFTR Folding and Endoplasmic Reticulum Associated-Degradation

Yoshihiro Matsumura, Larry L. David, and William R. Skach*

Department of Biochemistry and Molecular Biology

Oregon Health and Science University

Portland, OR 97239

Running Head: Essential role of Hsc70 on CFTR ERAD

*Address Correspondence to:
William R. Skach, M.D.,
L-224, 3181 SW Sam Jackson Park Road,
Portland, OR 97239
Phone: 503-494-7322
Fax: 503-494-8393
E-mail: skachw@ohsu.edu

A

Proteins	Plasmids	References
CBag	pProEx-CBag	Bhangoo *et al.*, 2007
E157A/K161A CBag	pProEx-CBag E157A/K161A	This work
Bag-1	pET15b-Bag-1	This work
Hsc70	pET15b-Hsc70	This work
Hsc70(229-309)	pET30-Hsc70(229-330)	This work
Hdj-2	pET28a-Hdj-2	Borges *et al.*, 2005
CHIP	pET30c-CHIP	Younger *et al.*, 2004
GST-CHIP	pGEX-4T.1-CHIP	This work
GST-Hsc70	pGEX-4T.1-Hsc70	This work

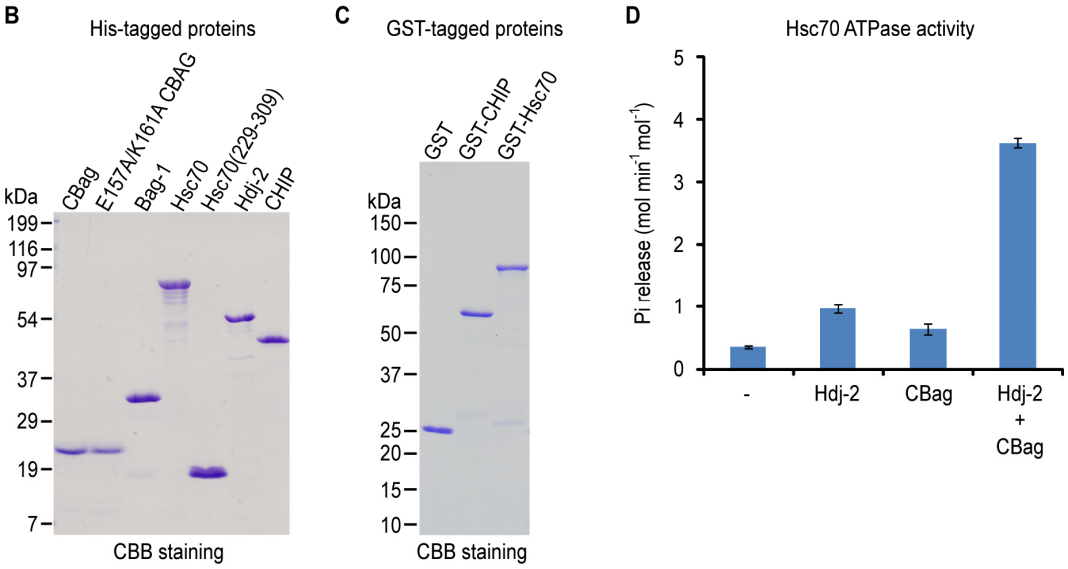

Supplemental Figure 1. Recombinant His and GST-tagged proteins.

(A) Table shows recombinant proteins and expression plasmids used in this study. (B) Each His-tagged protein was purified as described in *Supplemental Methods*, and 1 µg was separated on SDS-PAGE and stained with Coomassie Bryant Blue (CBB). (C) Each GST-tagged protein was purified as described in *Supplemental Methods*, and 1 µg was separated on SDS-PAGE and stained with CBB. (D) Steady state ATPase activity of recombinant His-tagged Hsc70 was measured as described in *Supplemental Methods.*

A

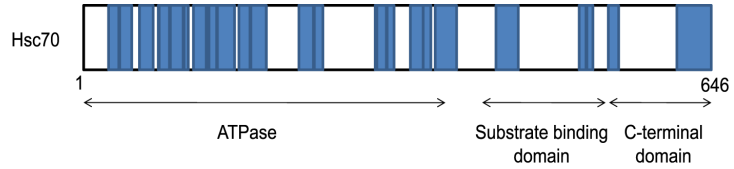

B

Sequence	Start (AA)	End (AA)	Number of spectra
(K)VEIIANDQGNR(T)	26	36	3
(R)TTPSYVAFTDTER(L)	37	49	1
(K)NQVAMNPTNTVFDAK(R)	57	71	3
(R)RFDDAVVQSDMK(H)	77	88	5
(R)FDDAVVQSDMK(H)	78	88	2
(K)HWPFMVVNDAGRPK(V)	89	102	2
(K)VQVEYKGETK(S)	103	112	1
(K)VQVEYK(G)	103	108	1
(K)SFYPEEVSSMVLTK(M)	113	126	3
(K)MKEIAEAYLGK(T)	127	137	3
(K)EIAEAYLGK(T)	129	137	1
(K)TVTNAVVTVPAYFNDSQR(Q)	138	155	3
(K)DAGTIAGLNVLR(I)	160	171	3
(R)IINEPTAAAIAYGLDK(K)	172	187	3
(R)IINEPTAAAIAYGLDKK(V)	172	188	4
(K)STAGDTHLGGEDFDNR(M)	221	236	3
(R)MVNHFIAEFK(R)	237	246	4
(R)ARFEELNADLFR(G)	300	311	3
(R)FEELNADLFR(G)	302	311	1
(R)GTLDPVEK(A)	312	319	2
(K)SQIHDIVLVGGSTR(I)	329	342	3
(K)LLQDFFNGK(E)	349	357	1
(K)SINPDEAVAYGAAVQAAILSGDK(S)	362	384	2
(K)QTQTFTTYSDNQPGVLIQVYEGER(A)	424	447	2
(R)LSKEDIER(M)	510	517	1
(R)MVQEAEK(Y)	518	524	1
(K)NSLESYAFNMK(A)	540	550	2
(K)LYQSAGGMPGGMPGGFPGGGAPPSGGASSGPTIEEVD(-)	610	646	1

Supplemental Figure 2. Identification of Hsc70 by mass spectrometry.

The 70-kDa band isolated from RRL by CBag affinity was excised from a silver stained gel and subjected to trypsinization and mass spectrometry analysis as described in *Supplemental Methods*. (A) Shown are regions of Hsc70 identified as trypsin fragments (in blue). (B) Unique sequences of 64 peptides identified by mass spectrometry analysis.

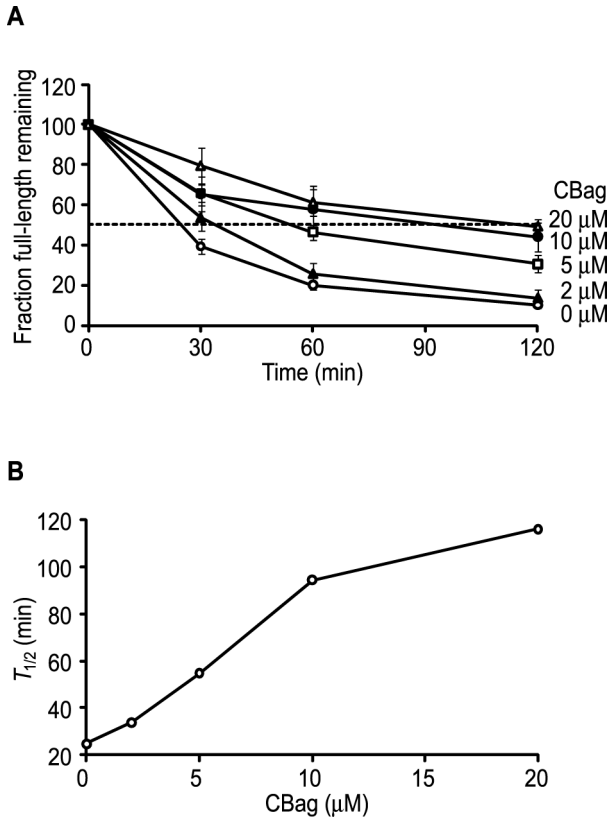

Supplemental Figure 3. CBag increases apparent $T_{1/2}$ of newly synthesized CFTR.

(A) Aliquots of degradation reactions were analyzed by SDS-PAGE. The fraction full-length CFTR remaining at each time point in the presence of indicated CBag concentration was determined by quantitating full-length CFTR band intensities using a phosphoimager (mean ± s.e.m., n = 3 to 7). (B) The graph shows the relationship between CBag concentration and apparent $T_{1/2}$ of full-length CFTR. $T_{1/2}$ is increased from 25 min to 116 min by 20 μM CBag. Note, however, that disappearance of full length CFTR band, which is typically reported in the literature, could reflect either conversion to ubiquitinated species, proteolytic cleavage, or both.

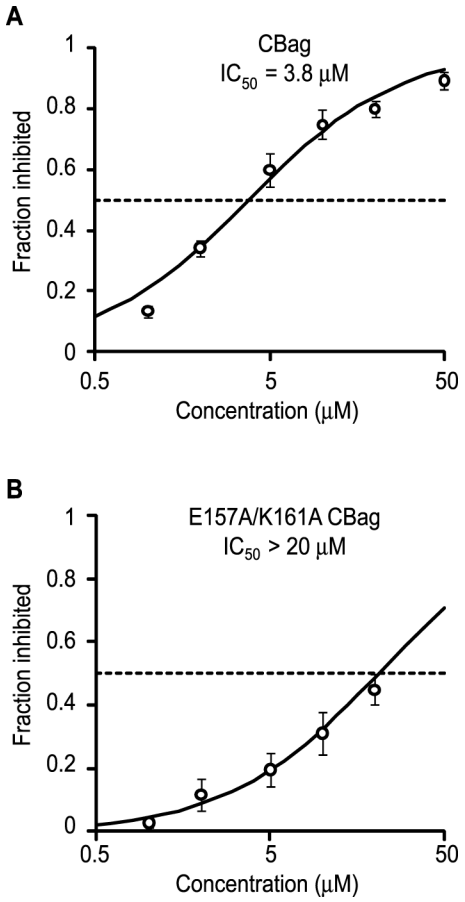

Supplemental Figure 4. Apparent IC_{50} values of CBag and E157A/K161A mutant CBag.

Data show the fraction of CFTR degradation (i.e. conversion into TCA-soluble peptides) that was inhibited by addition of wild-type CBag (A) or E157A/K161A CBag (B) calculated as described in *Supplemental Methods*. Line plotted shows least-squares fit to the equation $I = C/(IC_{50} + C)$ where I is the inhibition fraction (I = 1- % TCA sol $_{CBag}$ / % TCA sol; % TCA sol: control reaction without CBag; % TCA sol $_{CBag}$: reaction with CBag), C is the concentration of CBag (μM), and IC_{50} is the concentration that yields 50% inhibition in degradation. E157A/K161A CBag is >5 times less potent at inhibiting CFTR degradation than wild-type CBag.

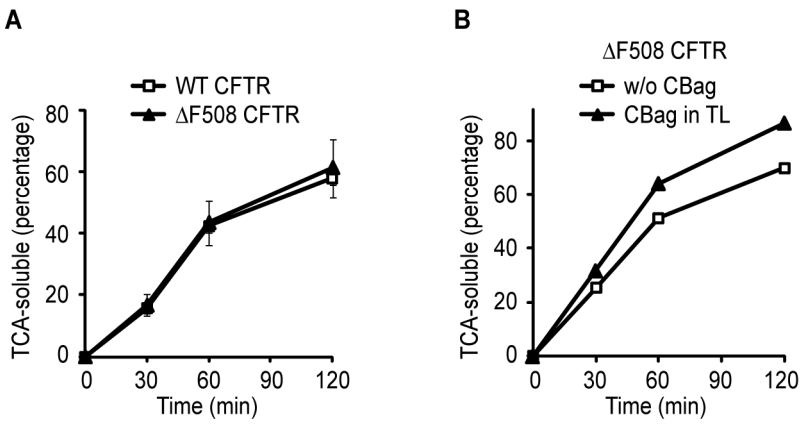

Supplemental Figure 5. Effect of CBag onΔF508 CFTR.

(A) Wild-type and ΔF508 CFTR were synthesized without CBag and subjected to *in vitro* degradation without CBag. Data shows mean ±s.e.m. (n = 3). (B) ΔF508 CFTR was synthesized with or without CBag and subjected to *in vitro* degradation without CBag. Result shows average of two independent experiments.

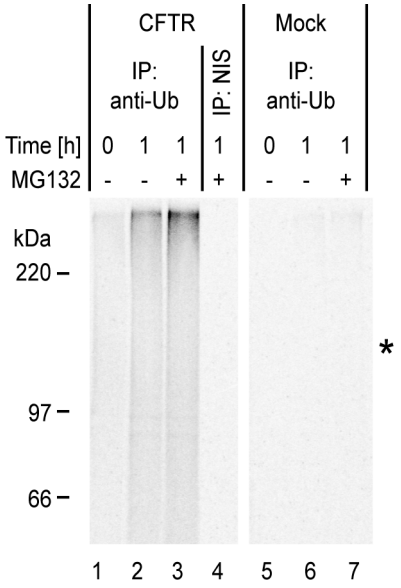

Supplemental Figure 6. Validation of CFTR ubiquitination.

Microsomes from translation reactions programmed with CFTR transcript (CFTT) or Mock transcript (Mock) were subjected to *in vitro* degradation with or without 100 μM MG132 as indicated. At T=1h, aliquots were immunoprecipitated with anti-(mono-/poly-) ubiquitin antibody (FK2) or non immune sera (NIS) and analyzed by SDS-PAGE and phosphorimaging. Size of full length CFTR is indicated by asterisk. Results verify that essentially all ubiquitinated radiolabled protein is derived from CFTR translation products.

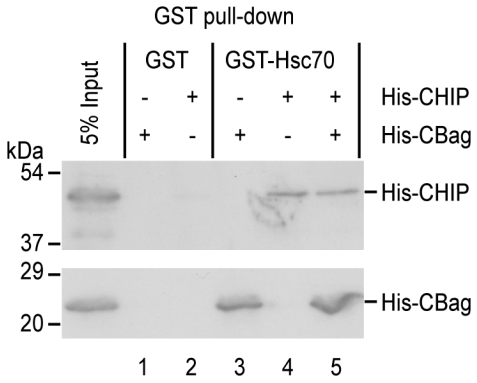

Supplemental Figure 7. CBag does not inhibit Hsc70-CHIP interaction *in vitro*.

Recombinant GST-Hsc70, His-CHIP, and/or His-CBag (4 μM) were incubated, and GST-Hsc70 was pull-downed with glutathione-uniflow resin. Bound proteins were eluted in 25 mM Tris-HCl, pH 7.5, 1 M NaCl, 1 mM β-mercaptoethanol, separated on SDS-PAGE, and subjected to immunoblotting with anti-CHIP or anti-CBag antisera.

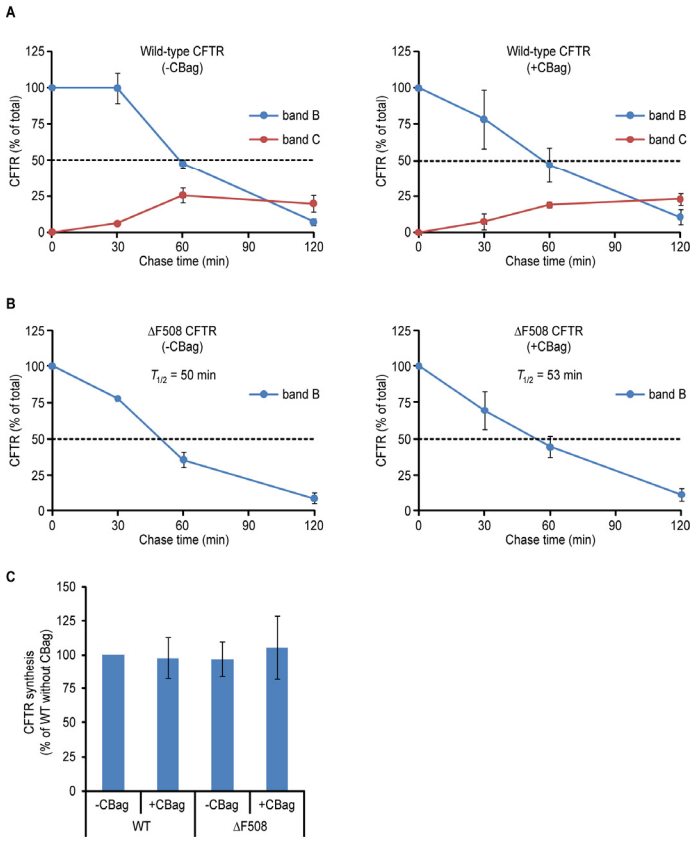

Supplemental Figure 8. Effects of CBag overexpression on CFTR maturation in HEK293 cells.

(A, B) Metabolic pulse-chase labeling experiments (30 min starvation, 15 min labeling, and 0 to 120 min chase) of wild-type and ΔF508 CFTR in HEK293 cells shown in Fig. 7C and D were quantified by phosphorimaging and normalized relative to the amount of band B at t = 0 min for each condition. Values are presented as mean ± s.e.m. (n = 3) for wild-type (A) and ΔF508 CFTR (B). (C) Effect of CBag overexpression on CFTR synthesis in HEK293 cells. Band B at t = 0 min (as in Fig 7 C and D) was quantified by phosphorimaging and normalized relative to the amount of band B in wild-type CFTR without CBag. Values are presented as mean ± s.e.m. (n = 4).

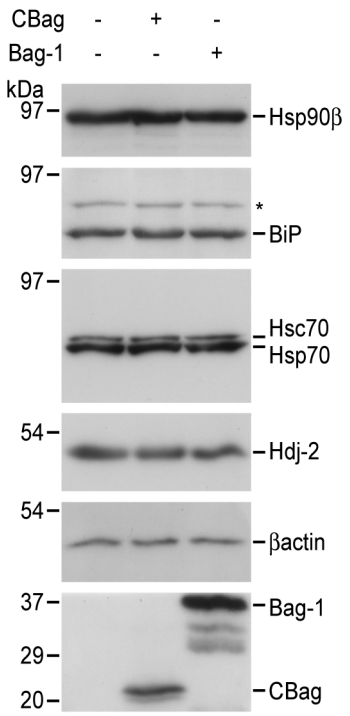

Supplemental Figure 9. Chaperone levels in HEK293 cells transfected with CBag or Bag-1.

Immunoblot of Hsp90β, BiP, Hsp/c70, and Hdj-2 whole cell lysate (25 μg) from transfected cells. Asterisk in BiP denotes a background band.

SUPPLEMENTAL METHODS

His and GST-tag Protein Expression and Purification

Recombinant proteins were expressed in E. coli BL21(DE3) transfected with appropriate plasmids (Supplemental Fig. 1A) by induction with 0.3 mM isopropyl β-D-1-thiogalactopyranoside (at A_{600} = 0.6) and incubation for 6 hours at 24 °C. His-tagged proteins were purified by TALON metal affinity or glutathione-uniflow resin (BD Biosciences, San Jose, CA) according to manufacturer's instruction followed by concentration on Centricon 10 kDa or 30 kDa cutoff (Millipore, Billerica, MA) with buffer replacement (protein storage buffer; 50 mM HEPES-NaOH, pH 7.5, 100 mM NaCl, and 1 mM DTT), flash frozen, and stored at −80 °C. Hdj-2 was purified and stored in the presence of 500 mM NaCl to prevent aggregation (Borges *et al.*, 2005). Proteins were at least 90–95% pure as confirmed by SDS-PAGE and Coomassie Brilliant Blue (CBB) staining (Supplemental Fig. 1B and C).

Steady State ATPase Activity of Recombinant Hsc70

Recombinant Hsc70 (5 μM) was incubated in 50 μl of 50 mM HEPES-NaOH (pH 7.5), 25 mM KCl, 5 mM $MgCl_2$, 0.1 mM EDTA, 0.5 mM DTT, and 3 mM ATP at 37˚C for 1 h +/– Hdj-2 and CBag (5 μM each) as indicated. TCA 1.7% (w/vol) was added to quench the reaction, followed by addition of ammonium molybdate (0.47% w/vol) and $SnCl_2$ (0.075% w/vol) at 25 °C for 20 min (Alder *et al.*, 2005). The phosphomolybdate concentration was measured spectroscopically (Abs_{800}) against a phosphate standard curve. ATPase activity of purified His-Hsc70 was 0.36 (min^{-1}), 0.96 (min^{-1}) in the presence of Hdj-2, and increased to 3.6 (min^{-1}) in the presence of both Hdj-2 and CBag (Supplemental Fig. 1C), in good

agreement with previous reports (Sondermann *et al.*, 2001; Tzankov *et al.*, 2008).

Mass Spectrometry Analysis

The CBag interacting 70-kDa band from RRL was excised from a silver stained gel, destained, and in-gel trypsin digested as previously described (Shibatani *et al.*, 2006). Extracted peptides were then analyzed by liquid chromatography-tandem mass spectrometry (LC-MS) using an LTQ linear ion trap (ThermoScientific, San Jose, CA) as previously described (Bassnet et al., 2009) except using a 60 min LC gradient. Peptide sequences were determined by comparing the observed MS/MS spectra to theoretical MS/MS spectra of peptides generated from a database using the program Sequest (Version 27, rev. 12, ThermoScientific). The database was constructed from rabbit, mouse, and human protein sequences derived from the SwissProt database (Swiss Institute of Bioinformatics) amended with identical but sequence reversed entries to estimate peptide and protein false discovery rates (77,358 total entries). Lists of identified peptides and proteins were then assembled using the program Scaffold (version 2_06_02, Proteome Software, Portland, OR). Thresholds for peptide and protein probabilities were set in Scaffold at 80 and 99.9%, respectively, and requiring a minimum of 2 peptides matched to each protein entry. Using these criteria, there were no matches to sequence reversed entries in the database.

IC_{50} of CFTR Conversion into Peptides for CBag

Apparent IC_{50} values of CFTR conversion into peptides for CBag were obtained from a graphical fit of the data using the equation $I = C/(IC_{50} + C)$ where C is the concentration of

CBag (μM) and *I* is the inhibition fraction. I = 1- [% TCA sol_{CBag} / % TCA sol] where % TCA sol is obtained from the control reaction without CBag and % TCA sol_{CBag} is obtained from the parallel reaction containing CBag.

In vitro Binding assay

For binding of GST-Hsc70, His-CBag, and His-CHIP, proteins (4 μM each) were incubated in 200 μL of 0.1% Triton X-100 in TBS at 4 °C for 1 hour. After addition of glutathione-uniflow resin (5 μL), samples were rotated for 1 hour at 4°C, washed 4 times with 0.1% Triton X-100 in TBS, twice with TBS, and eluted with 25 mM Tris-HCl, pH 7.5, 1 M NaCl, 1 mM β-mercaptoethanol. Eluates were separated on an SDS-PAGE gel and analyzed by immunoblotting.

SUPPLEMENTAL REFERENCES

Alder, N. N., Shen, Y., Brodsky, J. L., Hendershot, L. M., and Johnson, A. E. (2005). The molecular mechanisms underlying BiP-mediated gating of the Sec61 translocon of the endoplasmic reticulum. J. Cell Biol. *168,* 389-399.

Bassnett, S., Wilmarth, P. A. and David, L. L. (2009). The membrane proteome of the mouse lens fiber cell. Mol. Vis. *15,* 2448-2463.

Borges, J. C., Fischer, H., Craievich, A. F. and Ramos, C. H. (2005). Low resolution structural study of two human HSP40 chaperones in solution. DJA1 from subfamily A and DJB4 from subfamily B have different quaternary structures. J. Biol. Chem. *280*, 13671-13681.

Shibatani, T., Carlson, E. J., Larabee, F., McCormack, A. L., Früh, K. and Skach WR. (2006). Global organization and function of mammalian cytosolic proteasome pools: Implications for PA28 and 19S regulatory complexes. Mol. Biol. Cell. *17,* 4962-4971.

Sondermann, H., Scheufler, C., Schneider, C., Hohfeld, J., Hartl, F. U. and Moarefi, I. (2001). Structure of a Bag/Hsc70 complex: convergent functional evolution of Hsp70 nucleotide exchange factors. Science *291*, 1553-1557.

Tzankov, S., Wong, M. J., Shi, K., Nassif, C. and Young, J. C. (2008). Functional divergence between co-chaperones of Hsc70. J. Biol. Chem. *283*, 27100-27109.

Younger, J. M., Ren, H. Y., Chen, L., Fan, C. Y., Fields, A., Patterson, C. and Cyr, D. M. (2004). A foldable CFTRΔF508 biogenic intermediate accumulates upon inhibition of the Hsc70-CHIP E3 ubiquitin ligase. J. Cell Biol. *6*, 1075-1085.